temperature held at 45°C for 6 min, increased at 10°C min^{-1} to 130°C, increased at 5°C min^{-1} to 180°C, increased at 20°C min^{-1} to 230°C, held for 5 min, increased at 20°C min^{-1} to 250°C, and held for 5 min. Helium carrier gas flow was set to 1 ml min^{-1} with an electronic pressure control unit. Spectra were collected at −70 eV, and compounds were identified by comparison of retention times and mass spectra with those of authentic standards.

22. R. Halitschke, U. Schittko, G. Pohnert, W. Boland, I. T. Baldwin, *Plant Physiol.*, **125,** 711 (2001).
23. P. W. Pare, J. H. Tumlinson, *Phytochemistry* **47**, 521 (1998).
24. T. Koch, T. Krumm, V. Jung, J. Engelberth, W. Boland, *Plant Physiol*. **124**, 153 (1999).
25. A comparison of natural VOC emission with emissions from plants treated with individual VOCs as well as a detailed summary of observed and calculated values of top-down and bottom-up effects are available as supplementary data at *Science* Online at www.sciencemag.org/cgi/content/full/291/5511/2141/DC1.
26. We chose to attach *M. sexta* eggs on the underside of second and third stem leaves (measured from the bottom of the plant) to measure predation rates because an extensive study during the 1999 field season of mortality factors of both *Manduca* species revealed that predation rates depended on leaf position. The probability of predation for eggs and first to third instar hornworms on rosette leaves was 2.6 times higher than that on the second to fourth stem leaves and 11.8 times higher than that on the fifth or younger stem leaves (*29*). We followed the fate of 174 naturally oviposited hornworm eggs and could ascribe about 95% of the mortality to *G. pallens* predation. The decreasing predation rates of eggs and larvae feeding at higher leaf positions were likely due to the ground-dwelling behavior of *G. pallens*. We monitored the mortality of 559 naturally oviposited eggs in the 1999 field season, of which 71.75% were laid on first to fourth leaf position. About half of the mortality occurred at the egg stage (50.5%), 31.5% at first instar larvae, and 17.4% at second instar larvae (*29*).
27. Quantities of VOCs trapped for 7 hours from whole plants 24 hours after treatment with the α-cellulose glue used to fix eggs to leaves in the field experiment did not significantly increase any VOC emissions as compared with water-treated control plants (all *P* for compounds 1 to 7 >0.88). Laboratory experiments also demonstrated that naturally oviposited *M. sexta* eggs did not elicit a detectable plant VOC release in comparison with control plants without eggs (*29*).
28. We used 40- to 50-cm-tall flowering plants, growing 3 to 5 m apart in a 400-m linear transect across the population.
29. A. Kessler, unpublished results.
30. Supported by Max-Planck-Gesellschaft. We thank P. Feeny, J. Gershenzon, M. Hilker, J. McNeil, F. Roces, A. Roda, E. Wheeler, and three anonymous reviewers for helpful comments; B. Krock and H. Thomas for purifying the *cis*-α-bergamotene; R. Baumann for assistance with species determinations; and Brigham Young University for use of Lytle Preserve as a field station.

31 October 2000; accepted 6 February 2001

A Sperm Cytoskeletal Protein That Signals Oocyte Meiotic Maturation and Ovulation

Michael A. Miller,[1] Viet Q. Nguyen,[2] Min-Ho Lee,[3] Mary Kosinski,[1] Tim Schedl,[3] Richard M. Caprioli,[2] David Greenstein[1]*

Caenorhabditis elegans **oocytes, like those of most animals, arrest during meiotic prophase. Sperm promote the resumption of meiosis (maturation) and contraction of smooth muscle–like gonadal sheath cells, which are required for ovulation. We show that the major sperm cytoskeletal protein (MSP) is a bipartite signal for oocyte maturation and sheath contraction. MSP also functions in sperm locomotion, playing a role analogous to actin. Thus, during evolution, MSP has acquired extracellular signaling and intracellular cytoskeletal functions for reproduction. Proteins with MSP-like domains are found in plants, fungi, and other animals, suggesting that related signaling functions may exist in other phyla.**

In sexually reproducing metazoans, oocyte meiotic cell cycle progression is coordinated with ovulation and fertilization to ensure fusion of haploid gamete nuclei. In many animals, sperm trigger the resumption of meiosis in arrested oocytes, but the underlying mechanisms are not clear. During *C. elegans* reproduction, sperm promote oocyte meiotic maturation (M-phase entry) and gonadal sheath cell contraction, which act in concert to facilitate ovulation (*1*). Fertilization then occurs as ovulating oocytes enter a sperm storage compartment called the spermatheca (Fig. 1A). *Caenorhabditis elegans* sperm are separated from oocytes and sheath cells by a valve-like constriction of the distal spermatheca. Therefore, we reasoned that sperm likely secrete factors that promote both oocyte maturation and sheath contraction. To identify the sperm signals, we developed an in vivo bioassay by microinjecting sperm-conditioned medium (SCM) (*2*) into the uterus of *fog-2(q71)* females (*3*) (Fig. 1A). The oocyte maturation and sheath contraction rates are very low in these mutants (*1*), which lack sperm due to a defect in germline sex determination (*3*). Microinjection of SCM into *fog-2* females causes robust increases in the oocyte maturation and sheath cell contraction rates, as visualized by time-lapse video microscopy [Web movies (*4*)]. Sheath cells also respond with an increased contraction intensity, as measured by their lateral displacement. No activity is observed after the microinjection of bacterial extracts, female extracts, 1-methyladenine, serotonin, oxytocin, or M9 buffer.

The bioactive factors present in SCM are heat-resistant (100°C, 20 min) and sensitive to proteinase K digestion, suggesting that they are proteinaceous. Comparison of SCM to sperm lysates by SDS–polyacrylamide gel electrophoresis (SDS-PAGE) indicates that SCM is highly enriched with a single protein (Fig. 1B). The bioactive factors were purified with reversed-phase high-performance liquid chromatography (HPLC) using C_4 and C_{18} columns (*5*). Collected fractions were dialyzed in M9 buffer and assayed individually. Single peaks of maturation- and contraction-inducing activity elute from both columns (Fig. 1C). The identical separation characteristics of both activities on two columns with gradient elution indicates that both activities are likely contained in the same protein or protein complex. MALDI-TOF mass spectrometry shows that a polypeptide of 14,121 ± 1 dalton is present in the active fractions (Fig. 1D). Tryptic peptide mapping and sequencing representative fragments with post source decay mass spectrometry identify the bioactive polypeptide as the major sperm protein (MSP) (*6*). *Caenorhabditis elegans* MSP variants differing by one to four amino acids are encoded by a multigene family of approximately 40 genes (*7*). Closer analysis of the mass spectra reveals that several isoforms with similar molecular weights are present. Two of the major peaks match the calculated molecular weights of MSP-3 and MSP-142 (Fig. 1D). Nanomolar concentrations of SCM-purified MSP cause dramatic increases in the oocyte maturation and sheath cell contraction rates when microinjected into the uterus of *fog-2* females (Fig. 2). MSP, purified from sperm lysed with glass beads, produces identical signaling results and is indistinguishable from SCM-purified MSP by MALDI-TOF (*8*).

To verify that MSP is the signal for oocyte maturation and sheath contraction, we expressed and purified two MSP isoforms, MSP-77 and MSP-38, from *Escherichia coli* (*9*). Both isoforms, which differ by three amino acids, promote oocyte maturation and sheath contraction at rates equivalent to MSP

[1]Department of Cell Biology, [2]Mass Spectrometry Research Center, Vanderbilt University School of Medicine, Nashville, TN 37232, USA. [3]Department of Genetics, Washington University School of Medicine, St. Louis, MO 63110, USA.

*To whom correspondence should be addressed. E-mail: david.greenstein@mcmail.vanderbilt.edu

purified from sperm (Fig. 2). The optimal injected MSP concentration in the bioassay is 100 nM (Fig. 2, A through C), although the effective concentration in the female reproductive tract is likely much less because of dilution. Tonic sheath cell hypercontraction often results when concentrations of 200 or 400 nM are injected (Fig. 2B).

To test the hypothesis that MSP is the endogenous signal in wild-type animals, we injected antibodies to MSP into the uterus of adult hermaphrodites (*10*). This results in a reduction in the ovulation rate relative to control antibody injections [1.1 ± 0.3 ovulations per gonad arm per hour (n = 28) for antibodies to MSP versus 2.2 ± 0.3 ovulations per gonad arm per hour (n = 31) for control antibodies; $P < 0.001$]. Analysis of injected hermaphrodites using video microscopy indicates that the ovulation defect is due to a reduction in the oocyte maturation rate.

Sensing sperm availability is critical for reproduction in male-female nematode species, like *Caenorhabditis remanei*. The signal for ovulation in the genus *Caenorhabditis* is evolutionarily conserved because sperm from one species can promote ovulation in other species (*11*). Therefore, we tested whether *C. elegans* MSP could promote oocyte maturation and sheath contraction in *C. remanei* females. The injection of MSP-77 causes significant increases in the oocyte maturation and sheath contraction rates relative to the injection of buffer alone (Fig. 2).

These results strongly support the hypothesis that MSP is the signal that facilitates ovulation in *C. elegans* by promoting both oocyte maturation and sheath cell contraction. To determine how MSP signals these

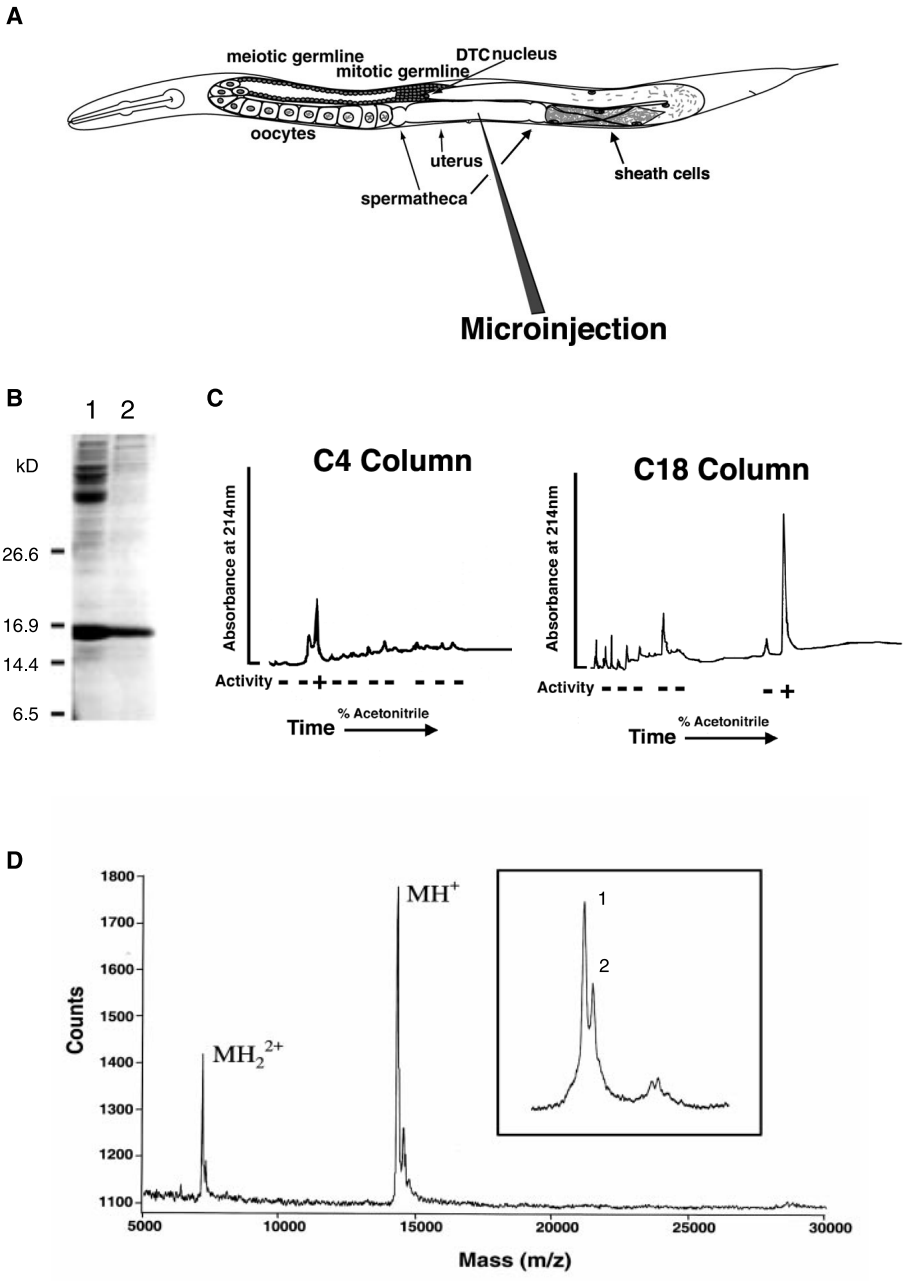

Fig. 1. Purification of the sperm signal. (**A**) Microinjection of SCM into the uterus of *fog-2* females. The gonad has two arms, and the germ line is shown in the anterior arm on the left, with the sheath encasing the germ line shown on the right. (**B**) SDS-PAGE analysis of lysed sperm (lane 1) and SCM (lane 2) showing enrichment of ~15-kD protein in SCM. (**C**) HPLC fractionation of SCM using C_4 and C_{18} columns. The oocyte maturation- and sheath contraction-inducing activities co-purified in a single peak of activity. (**D**) Mass spectrometry. The active fractions contained two peaks, a singly charged species (MH^+, MW = 14,121 ± 1 dalton) and a doubly charged species (MH_2^{2+}). The inset shows a higher resolution view of the MH+ peak, which consisted of a MW = 14,121 ± 1 dalton peak and a 14,1475 ± 1 dalton peak. Peak 1 corresponds to MSP-142 whereas peak 2 corresponds to MSP-3.

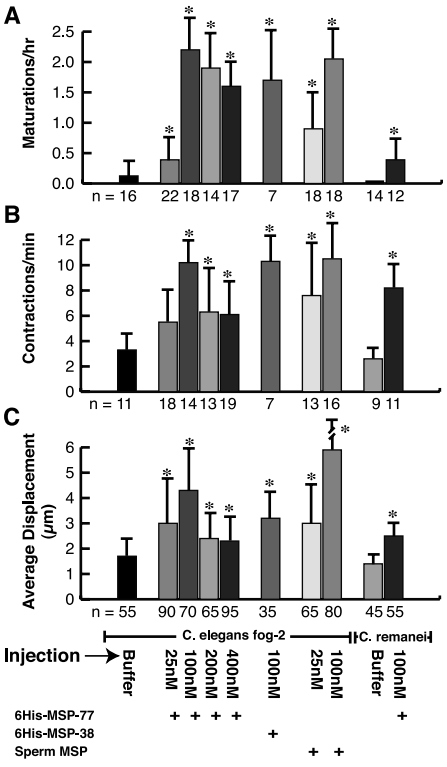

Fig. 2. MSP promotes oocyte maturation and sheath cell contraction. *Caenorhabditis elegans fog-2(q71)* or *C. remanei* females injected with MSP purified from sperm (Sperm MSP), 6His-MSP-77, and 6His-MSP-38 (two MSP isoforms differing by three amino acids) at different concentrations, or a buffer control. (**A**) Oocyte maturation rate per gonad arm. (**B**) Basal sheath contraction rate. (**C**) Maximal displacement of the sheath during contractions. Error bars indicate SD. The standard deviation of 100 nM sperm-purified MSP in (C) is 3.0. The values indicated by asterisks are significantly different ($P < 0.01$) than the buffer control by a two-sample t test. Values for n indicate the number analyzed. See Web video (*4*) for representative results.

two responses, we analyzed MSP deletion mutants. The COOH-terminal 20 amino acids of MSP are highly conserved among diverse nematodes (Fig. 3A). An MSP mutant lacking this COOH-terminal region [MSP(1 to 106)] promotes oocyte maturation, but not sheath cell contraction (Fig. 3, B through D). By contrast, a peptide (*12*) corresponding to the conserved COOH-terminal region [MSP(106 to 126)] promotes sheath cell contraction, but not oocyte maturation (Fig. 3, B through D). These results suggest that MSP has two separable signaling functions and likely activates distinct signal transduction pathways in oocytes and sheath cells.

Mitogen-activated protein kinase (MAPK) activation is a critical biochemical step in oocyte maturation in vertebrates (*13*). To determine if MAPK is activated in *C. elegans* oocytes during maturation, we stained dissected gonadal preparations of mated and unmated *fog-2* females with a monoclonal antibody against the activated, diphosphorylated form of MAPK (MAPK-YT) (*14*). This antibody stains the two to three most proximal oocytes only in the presence of sperm (Fig. 4, A and C). The MAPK-YT antibody only recognizes *mpk-1* MAP kinase gene products because no staining is observed in gonads from *mpk-1(ga117)* homozygotes (Fig. 4, I and J), a likely protein null (*15*). To determine whether MSP signaling is sufficient to activate MAP kinase in oocytes, we injected MSP into the uterus of females and stained with the MAPK-YT antibody (Fig. 4, E and G). This results in MAPK-YT staining in oocytes, indicating that MSP signaling activates the conserved MAP kinase cascade.

X-ray crystallography reveals that MSP folds into an immunoglobulin-like seven-stranded β sandwich, termed here the MSP domain, which is structurally related to the NH_2-terminal domain of the bacterial chaperonin, PapD (*16*). BLAST searches indicate that transmembrane proteins containing NH_2-terminal MSP-like domains are found in fungi, plants, and animals. These proteins, which are called VAMP-associated proteins (VAPs), appear to have diverse functions in somatic cells, including neurotransmitter release (*17*) and vesicle transport (*18*). The role of VAPs in germ cells is not known, but soluble *N*-ethylmaleimide–sensitive factor attachment protein receptor (SNARE) proteins, which can interact with VAPs during neurosecretion (*17*), have been implicated in fertilization in mammals (*19*) and sea urchins (*20*). To infer the evolutionary history of the sperm-specific MSPs and the more broadly expressed VAPs, we performed phylogenetic analyses using distance and parsimony methods. These results indicate that the VAP and MSP families form statistically well-supported, distinct monophyletic groups [Web fig. 1, (*4*)], suggesting that the MSP domain predates nem-

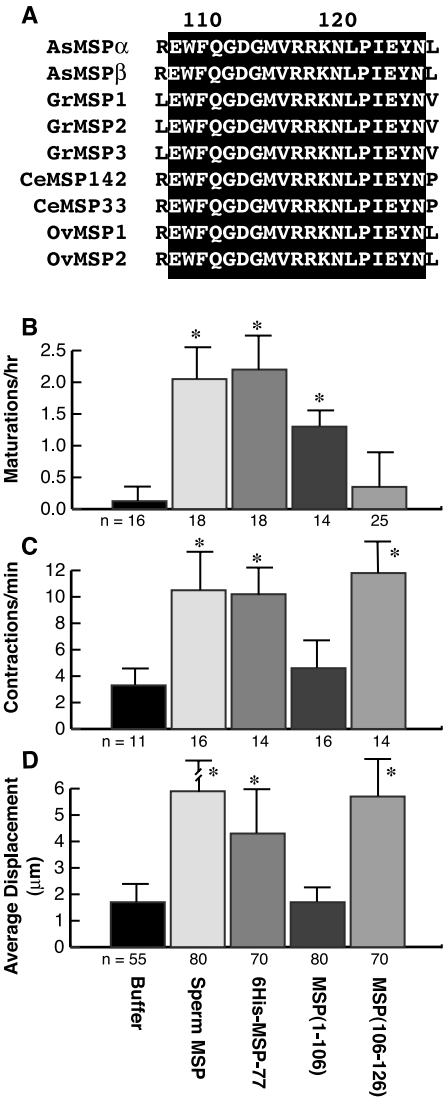

Fig. 3. Signaling activity of MSP deletion mutants. (**A**) Alignment of COOH-terminal MSP sequences (residues 106 to 126) from *Ascaris suum* (As) (GenBank accession numbers P27439 and P27440), the potato cyst nematode *Globodera rostochiensis* (Gr) (P53021, P53022, and AAA29148), *C. elegans* (Ce) (P53017 and P53019), and *Onchocerca volvulus* (Ov) (P13262 and P13263), which causes river blindness. (**B** through **D**) *Caenorhabditis elegans fog-2(q71)* females were injected with 100 nM MSP purified from sperm (Sperm MSP), 100 nM 6His-MSP-77, 100 nM MSP(1 to 106), 80 nM MSP- (106 to 126), or a buffer control. (B) Oocyte maturation rate per gonad arm. (C) Basal sheath contraction rate. (D) Maximal displacement of the sheath during contractions. Error bars indicate standard deviation. The standard deviation of 100 nM sperm-purified MSP in (D) is 3.0. The values indicated by asterisks are significantly different ($P < 0.01$) than the buffer control by a two-sample *t* test. Values for *n* indicate the number analyzed.

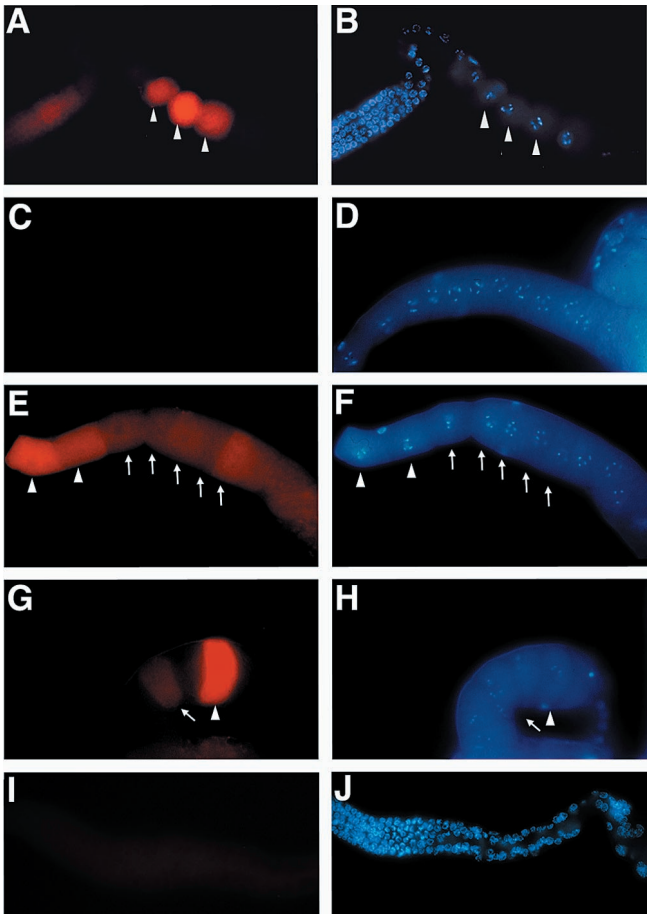

Fig. 4. MSP activates MAP kinase in oocytes. Activated MAP kinase (red) was observed in females that were mated (**A**) or injected with 100 nM 6-His-MSP-77 (**E** and **G**), but not in unmated females, which lack sperm (**C**). No staining is observed in *mpk-1(ga117)* hermaphrodites (**I**). DNA (blue) was visualized with 4′,6′-diamidino-2-phenylindole (DAPI) (**B**, **D**, **F**, **H**, and **J**). Arrowheads indicate oocytes that stain strongly and arrows indicate weakly staining oocytes. Proximal is to the right.

atodes. However, further interpretation of these phylogenetic analyses is complicated by two considerations. First, clear MSP orthologs have not been identified outside of nematodes. Second, some proteins involved in sexual reproduction have been observed to undergo rapid evolution (*21*), which could eclipse evolutionary relationships. Thus, the current data do not allow us to distinguish between two alternative models. One possibility is that MSP arose from VAP during the evolution of the nematode reproductive system and diverged, acquiring one or multiple new functions. Alternatively, MSP was present in the common ancestor of many animals and was lost in some lineages or remains to be identified. MSP signaling functions could be derived and unique to MSP, or ancestral and shared among MSP and some VAP homologs. In any event, the exceptionally high degree of conservation in nematodes makes MSP an attractive anti-helminthic drug target.

Nematode sperm use a pseudopod to move over short distances by crawling (*22*). MSP is the most abundant protein in sperm (*23*) and forms self-assembling filaments in the pseudopod (*24*). Unlike flagellar sperm found in many animals, nematode sperm contain essentially no actin (*25*) and crawling is thought to be dependent on MSP function (*26*). The mechanism by which MSP signals are delivered to oocytes and sheath cells is not currently understood and may be novel. MSP does not have a signal sequence nor do *C. elegans* sperm have ribosomes, an endoplasmic reticulum, or a Golgi system (*22*). Pseudopod formation is not required for MSP signaling because *spe-4* spermatocytes (*27*), which fail to form pseudopods, are still capable of promoting oocyte maturation and sheath contraction (*1*).

These results, taken together with previous studies (*24*), indicate that MSP has acquired both extracellular signaling and intracellular cytoskeletal functions during evolution. MSP appears to perform these functions by mediating multiple protein-protein interactions using its single immunoglobulin-like fold (*16*, *28*). The presence of MSP-like domains in yeast, plants, and animals suggests that some of these functions have been conserved during the evolution of multicellular organisms.

References and Notes

1. J. McCarter, B. Bartlett, T. Dang, T. Schedl, *Dev. Biol.* **205**, 111 (1999).
2. To prepare SCM, purified sperm (*23*) were incubated in M9 buffer ($\sim 5 \times 10^7$ sperm per milliliter) for 1 to 16 hours at 20°C. Sperm were removed by centrifugation and filtration through a 0.22-μm cellulose acetate filter. After microinjection (~50 pl), oocyte maturation and sheath cell contraction rates were monitored by time-lapse video microscopy (*1*) for 70 min.
3. T. Schedl, J. Kimble, *Genetics* **119**, 43 (1988).
4. Web movies 1 through 4 and Web fig. 1 are available at *Science* Online at www.sciencemag.org/cgi/content/full/291/5511/2144/DC1.
5. SCM or sperm lysates, prepared by vortexing with glass beads, were fractionated on C_4 and C_{18} columns (Vydac, Hesperia, CA) using an acetonitrile gradient (0 to 100%) mobile phase containing 0.1% trifluoroacetic acid. Absorbance peaks (214 nm) were collected manually, dialyzed against M9, and bioassayed.
6. Active fractions were analyzed by MALDI-TOF mass spectrometry. Post source decay mass spectrometry (*29*) of a 1960-dalton peptide, generated by tryptic digestion of the active fraction, yielded the sequence IVFNAPYDDKHTYHIK (*30*), matching MSP.
7. S. Ward *et al.*, *J. Mol. Biol.* **199**, 1 (1988).
8. M. Miller, V. Nguyen, R. Caprioli, D. Greenstein, unpublished data.
9. His-tagged MSP-77, MSP-38, and MSP(1 to 106) were purified under native conditions by Ni–nitrilotriacetic acid (Ni-NTA) (Qiagen, Valencia, CA) affinity chromatography (>99% pure by SDS-PAGE and MALDI-TOF). MSP concentrations were determined by amino acid hydrolysis, SDS-PAGE, and spectrophotometrically using ε (275 nm) = 3.29×10^4 M^{-1} cm^{-1}.
10. Antibodies to MSP (*23*) or EMB-30 control antibodies were injected (~40 μg/ml) into wild-type adult hermaphrodites (24 hours post-L4 at 20°C), which were then cultured individually with food for 3 hours. Total ovulations were determined (*1*) and oocyte maturation was analyzed by time-lapse video microscopy. A two-sample *t* test was used to assess statistical significance.
11. K. L. Hill, S. W. L'Hernault, *Dev. Biol.* **232,** 105 (2001).
12. The COOH-terminal MSP peptide (REWFQGDGMVRRKNLPIEYNP) (*30*) was prepared by solid-phase synthesis and purified by HPLC.
13. J. E. Ferrell Jr., *Bioessays* **21**, 833 (1999).
14. Diphosphorylated MPK-1 was detected using indirect immunofluorescence with the antibody MAPK-YT (*31*) (Sigma). Dissected and fixed (3% paraformaldehyde) gonads were stained 40 min post MSP injection.
15. M. R. Lackner, S. K. Kim, *Genetics* **150**, 103 (1998).
16. T. L. Bullock, T. M. Roberts, M. Stewart, *J. Mol. Biol.* **263**, 284 (1996).
17. P. A. Skehel, K. C. Martin, E. R. Kandel, D. Bartsch, *Science* **269**, 1580 (1995).
18. L. Soussan *et al.*, *J. Cell Biol.* **146**, 301 (1999).
19. J. Ramalho-Santos *et al.*, *Dev. Biol.* 223, 54 (2000).
20. J. R. Schulz, J. D. Sasaki, V. D. Vacquier, *J. Biol. Chem.* **273**, 24355 (1998).
21. V. D. Vacquier, *Science* **281**, 1995 (1998).
22. S. W. L'Hernault, in *C. elegans II*, D. L. Riddle, T. Blumenthal, B. J. Meyer, J. R. Priess, R., Eds. (Cold Spring Harbor Laboratory Press, Cold Spring Harbor, NY, 1997), pp. 271–294.
23. M. R. Klass, D. Hirsh, *Dev. Biol.* **84**, 299 (1981).
24. T. M. Roberts, M. Stewart, *J. Cell Biol.* **149**, 7 (2000).
25. G. A. Nelson, T. M. Roberts, S. Ward, *J. Cell Biol.* **92**, 121 (1982).
26. J. E. Italiano Jr., T. M. Roberts, M. Stewart, C. A. Fontana, *Cell* **84**, 105 (1996).
27. S. W. L'Hernault, P. M. Arduengo, *J. Cell Biol.* **119**, 55 (1992).
28. H. E. Smith, S. Ward, *J. Mol. Biol.* **279**, 605 (1998).
29. R. Kaufmann, B. Spengler, F. Lutzenkirchen, *Rapid Comm. Mass Spectrom.* **7**, 902 (1993).
30. Single-letter abbreviations for the amino acid residues are as follows: A, Ala; C, Cys; D, Asp; E, Glu; F, Phe; G, Gly; H, His; I, Ile; K, Lys; L, Leu; M, Met; N, Asn; P, Pro; Q, Gln; R, Arg; S, Ser; T, Thr; V, Val; W, Trp; and Y, Tyr.
31. Y. Yung *et al.*, *FEBS Lett.* **408**, 292 (1997).

32. We thank S. Ward for providing antibodies and Y. Kohara for expressed sequence tag clones. Some strains used in this study were provided by the *Caenorhabditis* Genetics Center, which is supported by NIH. We thank D. Bridge, C. Desai, B. Hogan, D. Miller, and R. Steele for helpful discussions and review of the manuscript. We thank E. Mitchell for digital video editing. M.A.M. and M.K. were supported by NIH training grants HD07043 and CA09592. Supported by grants from NIH (GM57173 to D.G., GM58008 to R.M.C., and HD25614 to T.S.).

20 November 2000; accepted 7 February 2001

Sonic Hedgehog Control of Size and Shape in Midbrain Pattern Formation

Seema Agarwala, Timothy A. Sanders, Clifton W. Ragsdale*

Little is known about how patterns of cell types are organized to form brain structures of appropriate size and shape. To study this process, we employed in vivo electroporation during midbrain development to create ectopic sources of Sonic Hedgehog, a signaling molecule previously shown to specify different neuronal cell types in a concentration-dependent manner in vitro. We provide direct evidence that a Sonic Hedgehog source can control pattern at a distance in brain development and demonstrate that the size, shape, and orientation of the cell populations produced depend on the geometry of the morphogen source. Thus, a single regulatory molecule can coordinate tissue size and shape with cell-type identity in brain development.

The determination of cell fate and the spatial organization of differentiated cells are the fundamental processes by which any tissue is organized during development. An attractive mechanism for achieving spatial patterns of different neuronal cell types is through a "positional signal" from a morphogen source that elicits distinct molecular responses in target cells according to their distance from that source (*1, 2*). Evidence that Sonic Hedgehog (SHH) can serve as a positional signal in vertebrate central nervous system (CNS) development has come mainly from in vitro studies demonstrating that different cell

Department of Neurobiology, Pharmacology, and Physiology, The University of Chicago, Chicago, IL 60637, USA.

*To whom correspondence should be addressed. E-mail: cliff@drugs.bsd.uchicago.edu